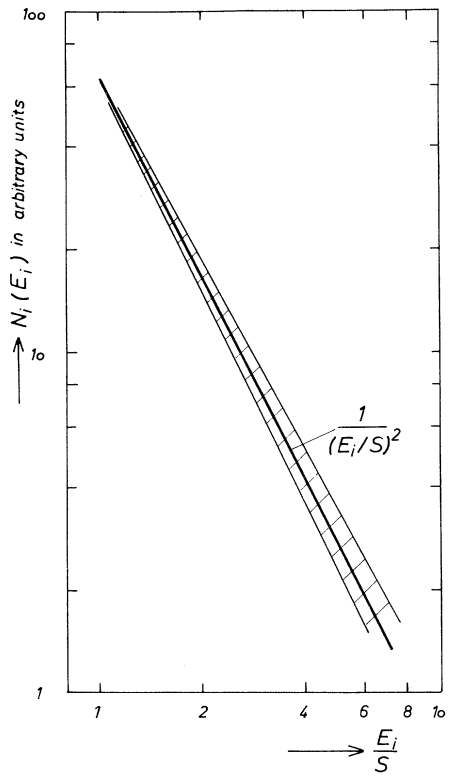

FIG. 1. Energy distribution functions $N_I(E_I)$ of the recoil atoms within the solid plotted versus the reduced energy E_I/S. All $N_I(E_I)$ curves for the different target elements appear in the hatched region and are compared with the $(E_I/S)^{-2}$ curve indicated by the solid line.

energies for those particles emitted in the 45° direction from polycrystalline and monocrystalline Au and Cu under high energy ion bombardment. Taking into account the different direction under observation compared with that in the present work, it can be concluded that by the bombardment of a polycrystalline solid with ions at energies ranging upwards from approximately 1 keV, a random collision cascade is produced with an isotropic spectral flux density $N_I(E_I)$, which decreases in a wide range as E_I^{-2}.

More information on the evaluation processes for obtaining $N(E)$ and then $N_I(E_I)$, and the complete results with a more detailed discussion, will be found in another paper, which will be submitted elsewhere.[8]

The author is gratefully indebted to Professor Dr. W. Hink for his encouraging interest and to the Deutsche Forschungsgemeinschaft for financial support in this work.

[1]M. W. Thompson, Phil. Mag. 18, 377 (1968).
[2]E. Hulpke and Ch. Schlier, Z. Physik 207, 294 (1967).
[3]H. Beuscher and K. Kopitzki, Z. Physik 184, 382 (1965).
[4]R. V. Stuart and G. K. Wehner, J. Appl. Phys. 35, 1819 (1964).
[5]R. V. Stuart, G. K. Wehner, and G. S. Anderson, J. Appl. Phys. 40, 803 (1969).
[6]H. Oechsner and L. Reichert, Phys. Letters 23, 90 (1966).
[7]H. Oechsner, in Proceedings of the Eighth International Conference on the Phenomena in Ionized Gases, Vienna, 1967 (Springer, Berlin, 1967).
[8]H. Oechsner, to be published.

EMISSION IN THE REGION 4000 TO 7000 Å VIA FOUR-PHOTON COUPLING IN GLASS

R. R. Alfano and S. L. Shapiro
Bayside Research Center of General Telephone & Electronics Laboratories Incorporated,
Bayside, New York 11360
(Received 9 January 1970)

Four-photon stimulated scattering has been observed in borosilicate glass under high-power 5300-Å picosecond-pulse excitation. Parametric emission is generated from 4000 to 7000 Å from filaments formed in the glass, the wavelength depending on the emission angle.

We report the first observation of nondegenerate four-photon stimulated emission in glass originating in filaments created under high-power, 5300-Å, picosecond-pulse excitation.

The four-photon coupling process originates through the electronic distortion of molecules inside self-trapped filaments in the material. Positive and negative frequency sweeps are generated inside the filaments[1] and the frequency-swept photons and laser photons are coupled to the laser field via the third-order susceptibility χ^3 or intensity-dependent dielectric constant $\epsilon_2 E^2$. The four-photon process is of the type $\vec{K}_0 + \vec{K}_0 = \vec{K}_1 + \vec{K}_{-1}$ where $\vec{K}_0$, $\vec{K}_1$, and $\vec{K}_{-1}$ are the wave vectors of the laser beam, Stokes-shifted photons, and anti-Stokes-shifted photons, respectively. Chiao,

Kelley, and Garmire[2] have shown theoretically that when weak Stokes and anti-Stokes waves accompany a strong laser wave, both Stokes and anti-Stokes waves are amplified via χ^3. This implies four-photon parametric oscillation. Degenerate four-photon interactions in liquids and the interaction with the Rayleigh wing were first described by Chiao, Kelley, and Garmire[2] and observed by Carman, Chiao, and Kelley.[3]

Amplification of Stokes and anti-Stokes waves found in this investigation is different from the Raman process.[4,5] This process cannot be a two-step Raman process requiring coherent optical phonons as an intermediate step because there are no sharp molecular vibrations in borosilicate BK-7 glass, and because Stokes emission appears of about equal intensity to the anti-Stokes emission. The appearance of Stokes emission is in sharp contrast to results[5] that show that the Raman process in a liquid is a two-step process with intermediate optical phonons involved and with no Stokes radiation observed at the matching angle. The emission frequency in the Raman process is well defined, while in the four-photon process the frequency is shifted continuously from 0 to as much as 6000 cm^{-1} on both the Stokes and anti-Stokes sides. Our process requires a modulation of the electronic polarization.

In the present experiment picosecond light pulses at 1.06 μ are generated from a dye Q-switched Nd:glass mode-locked laser. Second-harmonic generated (SHG) pulses at 5300 Å are derived by passing the beam through a potassium dihydrogen phosphate (KDP) crystal cut at the phase-matched angle. SHG pulses only are then collimated with an inverted telescope to a diameter of 1.2 mm and then passed through the samples. The energy per pulse is ~5 mJ and the pulse length is 4-8 psec so that the power is ~1 GW/cm^2. Five to ten filaments about 20 μ in diameter are formed in the sample so that the power in the filaments could be as high as ~10^4 GW/cm^2.

Emission from the sample is displayed as a function of angle and wavelength by placing a lens at the focal distance from the 2-cm-high slit of a $\frac{3}{4}$-m Jarrell-Ash spectrograph. The sample is near the lens so that light at a given wavelength emerging at the same angle with respect to the laser beam is imaged in a ring on the spectrograph slit. Anti-Stokes shifted light is displayed by placing either one or two 5-60 Corning filters before the lens to attenuate the main laser beam. Stokes light is displayed in an analogous fashion except that three 3-67 and three 3-68 filters are used to attenuate the main 5300-Å beam.

An anti-Stokes spectrum emitted from borosilicate BK-7 glass is shown in Fig. 1(a). The light is focused on the slit with a 10-cm focal length lens with the laser beam position at the center of the slit and the spectrograph turned to the second order. The whole anti-Stokes spectrum is displayed with the spectrograph operating in the first order as shown in Fig. 1(b). The laser-beam position in Fig. 1(b) is near the bottom of the slit so that only the upper half of the anti-Stokes curve is displayed. In this fashion the entire angular variation of the anti-Stokes spectrum is displayed since the spectrum does not go off the slit at large emission angles.

Three salient features are evident in the spectra shown in Fig. 1. The first is four-photon continuous emission of radiation in the form of a curve extending from 4000 to 5300 Å, a shift of 6000 cm^{-1}. The second feature is the forward-scattered frequency-swept radiation indentified previously.[1] The third feature is the conical light emission which seems to begin near the forward direction at about 1000-cm^{-1} shift from the main laser line (it may possibly start at 0-cm^{-1} shift) and extends to 6000 cm^{-1}. This third feature is not yet understood but could possibly be frequency-swept light at small angles to the beam axis. This explanation is plausible in part because frequency-swept light at small angles could help to trigger the four-photon process. A similar spectral curve also appears on the Stokes side from 5300 to 7000 Å. Stimulated emission thus occurs over the entire visible region.

One outer curve which fluctuates in angle by

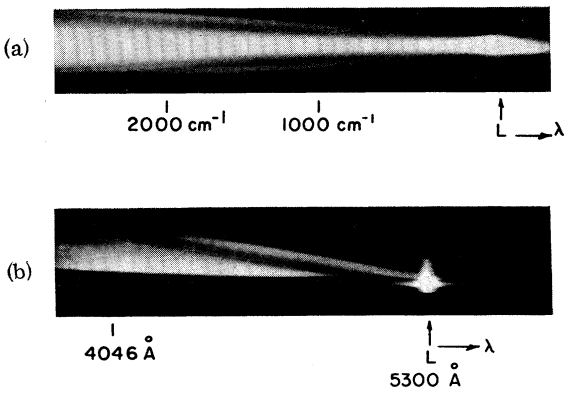

FIG. 1. (a) Anti-Stokes emission with main laser beam at slit center. Light in center is frequency swept light while outer curves is due to four-photon emission. (b) Entire angular anti-Stokes emission curve from 4000 to 5300 Å.

about 10% at a given frequency always appears, and this is the curve we analyze. One important experimental observation is that emission at a particular wavelength varies in emission angle from shot to shot. Also curves do not usually go to zero angle at zero frequency shift. The experimental angle φ_1 varies from ~0.01 to 0.03 at zero frequency shift from shot to shot. On the same shot the angular width of emission at a given frequency can be as large as $\Delta\varphi_1 \sim 0.02$ although it can be less than $\Delta\varphi_1 \sim 0.01$. Also experimentally extra curves of smaller diameter are often observed from shot to shot.

Historically two types of anti-Stokes radiation have been reported. Class-I radiation was first observed in calcite[6] and obeys the volume phase-matching equation $\vec{K}_0 + \vec{K}_0 = \vec{K}_1 + \vec{K}_{-1}$. Class-II radiation fails to obey the volume phase-matching relation and originates in filaments.[7] Detailed explanations of anti-Stokes radiation from filaments have been given by Shimoda[8,9] and Sacchi, Townes, and Lifsitz.[10]

In Fig. 2 different four-photon scattering processes are compared with one of our experimentally measured curves. The first curve labeled I is calculated for volume phase matching where $2\vec{K}_0 = \vec{K}_1 + \vec{K}_{-1}$. Refractive indices for borosilicate BK-7 glass are known accurately to five decimal places,[11] and thus the calculated curve is accurate. Class radiation originates either from phase matching over a large volume or from phase matching in large-diameter filaments. Curve I deviates from the experimental curve for two main reasons: (1) the light is formed in small filaments of diameter ~20 μ and (2) high-power short-pulse lasers which are multimode induce a nonlinear refractive index change in the material. The Class-I model correctly predicts one qualitative feature, however—the greater angle of emission at a given frequency shift for the Stokes curve than for the anti-Stokes curve and by about the right amount, i.e., $\varphi_{-1} = (K_1/K_{-1})\varphi_1$ at small angles where φ_{-1} is the Stokes emission angle and φ_1 is the anti-Stokes emission angle.

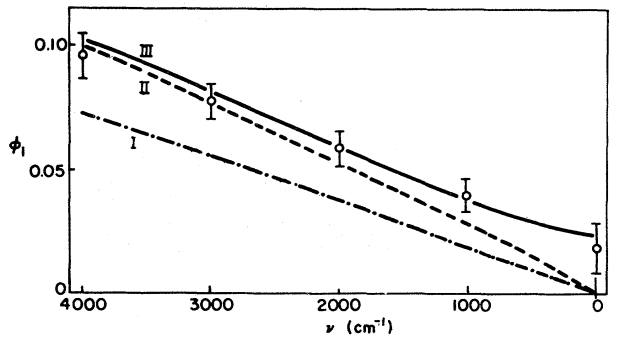

FIG. 2. Anti-Stokes angle outside material: circles, experimental points; dash-dot, curve I calculated for Class-I emission; dash, curve II calculated for Class-II emission; solid line, curve III calculated for small scale filaments plus a nonlinear index change.

The curve labeled II in Fig. 2 is a calculated curve for Class-II emission from small-scale filaments. Following Shimoda[8] the anti-Stokes angle φ_1 is calculated from

$$\varphi_1^2 = 2\Delta K_1/K_1 - a^2/2l^2, \tag{1}$$

where $\Delta K_1 = K_1 + K_{-1} - 2K_0$, $2a$ is the filament diameter, and l is the filament length. Unfortunately it is not clear which values to use for a/l. Taking $a = 10$ μ and $l = 2$ mm to 1 cm, which are typical experimental values, the term $a^2/2l^2$ is small compared with $2\Delta K_1/K_1$. As shown in Fig. 2, the curve labeled II and calculated from $\varphi_1^2 = 2\Delta K_1/K_1$ is much closer to the experimental data than the volume phase-matching curve labeled I.

An important correction to the emission angle is produced by the nonlinear change of refractive index induced by the short, intense laser pulses. This correction tends to increase both anti-Stokes and Stokes emission angles and is most important at small angles. Chiao, Kelley, and Garmire[2] have shown that the refractive index increase for weak waves is twice that of the strong wave. Thus instead of Eq. (1) for the radiation angle for the filaments we write a new ΔK_1, $\Delta K_1'$, which takes into account the nonlinear increase in refractive index, i.e., $\Delta K_1' = K_1 + 2\Delta K + K_{-1} + 2\Delta K - 2K_0 - 2\Delta K$ so that

$$\varphi_1^2 = \frac{2\Delta K_1}{K_1} + \frac{4\Delta K}{K_1} - \frac{a^2}{2l^2}, \tag{2}$$

where $\Delta K = \Delta n \omega_0/c$ and Δn is the change of refractive index induced by the intense pulse. The electronic index change Δn for the strong wave is $\frac{3}{8}\epsilon_2 E_0^2/n_0$ while for the weak wave Δn is $\frac{3}{4}\epsilon_2 E_0^2/n_0$ where ϵ_2 is the electronic Kerr coefficient. For a laser pulse which changes n for the strong wave by 10^{-4}, Eq. (2) is plotted in Fig. 2. This curve, labeled III, provides an excellent fit to the experimental data and is a reasonable model because it takes into account both that the radiation pattern is from filaments and that the refractive index increases as a result of short, intense pulses. Equation (2) provides an explanation of the finite emission angle observed at zero frequency shift because of the refractive index

increase. Fluctuations in emission angle from shot to shot as well as the extra curves observed experimentally could be explained by the $a^2/2l^2$ and $4\Delta K/K_1$ terms in Eq. (2) which vary for different filaments.

This process is quite general and we have observed similar curves in other glasses, calcite, and liquids such as methanol and acetone. Borosilicate glass is chosen for specific analysis because accurate values of the refractive index are available and because there are no sharp vibrational Raman lines which would interfere with the interpretation of a four-photon nondegenerate process. We do observe Class-II Raman rings from calcite and the liquids.

The four-photon coupling mechanism in borosilicate glass is surely electronic, but in liquids a possible coupling mechanism could be the optical orientational Kerr effect, although this mechanism appears to be ruled out since the spectral extents in liquids are thousands of wave numbers which is much greater than the inverse of the orientational relaxation times. In view of experimental complications—i.e., short intense pulses, filaments, self-phase modulation—agreement between experiment and theory is excellent.

Four-photon parametric oscillation should be enhanced by placing resonator mirrors at the Stokes or anti-Stokes emission angles. Four-photon processes are probably present inside Q-switched and mode-locked Nd:glass lasers and thus influence laser action.

We thank Dr. A. Lempicki for helpful discussions, Dr. H. Samelson for a critical reading of the manuscript, and S. Hussain for technical assistance.

[1]R. R. Alfano and S. L. Shapiro, Phys. Rev. Letters 24, 592 (1970) (this issue).
[2]R. Y. Chiao, P. L. Kelley, and E. Garmire, Phys. Rev. Letters 17, 1158 (1966).
[3]R. L. Carman, R. Y. Chiao, and P. L. Kelley, Phys. Rev. Letters 17, 1281 (1966).
[4]E. Garmire, F. Pandarese, and C. H. Townes, Phys. Rev. Letters 11, 160 (1963).
[5]H. J. Zeiger, P. E. Tannenwald, S. Kern, and R. Herendeen 11, 419 (1963).
[6]R. Y. Chiao and B. P. Stoicheff, Phys. Rev. Letters 12, 290 (1964).
[7]E. Garmire, thesis, Massachusetts Institute of Technology, 1965 (unpublished).
[8]K. Shimoda, Japan. J. Appl. Phys. 5, 86 (1966).
[9]K. Shimoda, Japan. J. Appl. Phys. 5, 615 (1966).
[10]C. A. Sacchi, C. H. Townes, and J. R. Lifsitz, Phys. Rev. 174, 439 (1968).
[11]Optical Glass Tables, Jena Glaswerk Schott and Gen, Mainz, Germany, p. 18.

COMMENTS ON "LORENZ-FUNCTION ENHANCEMENT DUE TO INELASTIC PROCESSES NEAR THE NÉEL POINT OF CHROMIUM"*

J. P. Moore, R. K. Williams, and D. L. McElroy
Metals and Ceramics Division, Oak Ridge National Laboratory, Oak Ridge, Tennessee 37830
(Received 10 October 1969)

A peak has been reported in the thermal conductivity (and hence the Lorenz function) of Cr at the Néel temperature. The investigators reporting this effect have ignored a considerable body of previous results on several chromium specimens. None of the previous results indicate a peak in the thermal conductivity. We feel that the effect is suspect and may be associated with defects in experimental technique.

A recent paper by Meaden, Rao, and Loo[1] reports the existence of a sharp peak in the Lorenz function of chromium at the Néel temperature. They propose that this effect is caused by an enhanced electronic thermal conductivity from a reduction of electron scattering by phonons. MRL imply that this effect was not observed in our prior measurements[2,3] on three Cr samples either because the measurements were made without "quite high resolution and precision" or because of the larger temperature differences which we employed. Until some stronger evidence is reported, we feel that their results are suspect for several reasons.

Although their electrical resistivity (ρ) values are in good agreement with the data which we reported for our "A" sample, the thermal conductivity (λ) results disagree as shown in Fig. 1. As noted on Fig. 1 we made two series of measurements with gradients of approximately 0.4 deg cm^{-1} (approximately 1.4-deg total ΔT between temperature sensors) and 1.4 deg cm^{-1} (approximately 5-deg ΔT). All our data are within $\pm 0.7\%$ of a smooth curve, show no dependence

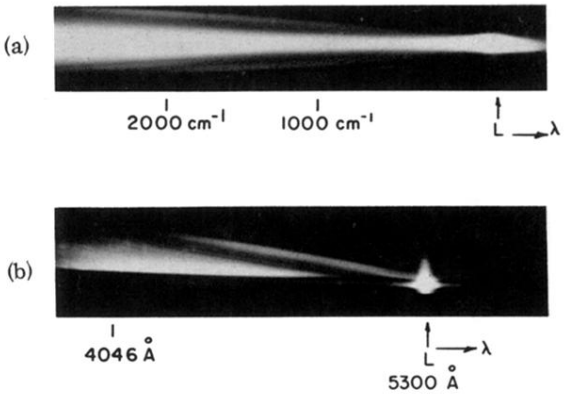

FIG. 1. (a) Anti-Stokes emission with main laser beam at slit center. Light in center is frequency swept light while outer curves is due to four-photon emission. (b) Entire angular anti-Stokes emission curve from 4000 to 5300 Å.